

Has the GZK suppression been discovered?

John N. Bahcall^{a,1} and Eli Waxman^{b,2}

^a*School of Natural Sciences, Institute for Advanced Study, Princeton, NJ 08540, USA*

^b*Physics Faculty, Weizmann Institute of Science, Rehovot 76100, Israel*

Abstract

The energy spectra of ultra high energy cosmic rays reported by the AGASA, Fly's Eye, Haverah Park, HiRes, and Yakutsk experiments are all shown to be in agreement with each other for energies below 10^{20} eV (after small adjustments, within the known uncertainties, of the absolute energy scales). The data from HiRes, Fly's Eye, and Yakutsk are consistent with the expected flux suppression above 5×10^{19} eV due to interactions of cosmic rays with the cosmic microwave background, the Greisen-Zatsepin-Kuzmin (GZK) suppression, and are inconsistent with a smooth extrapolation of the observed cosmic ray energy spectrum to energies $> 5 \times 10^{19}$ eV. AGASA data show an excess of events above 10^{20} eV, compared to the predicted GZK suppression and to the flux measured by the other experiments.

1 Introduction

We analyze the observed spectrum of ultra-high energy cosmic rays. We find two main results: (i) The energy spectra reported by the AGASA, Fly's Eye, Haverah Park, HiRes and Yakutsk experiments are all in good agreement for energies below 10^{20} eV, and (ii) All the data are consistent with a GZK suppression except for the AGASA points above 10^{20} eV. Our principal conclusion from these two results is that standard physics, including the GZK suppression, is sufficient to explain all of the existing data on UHE cosmic rays.

For any theoretical model in which the GZK suppression is present, the assumed intrinsic spectrum produced by the UHE cosmic-ray sources influences the energy spectrum predicted by the model. Our conclusion that the data

¹ E-mail: jnb@sns.ias.edu

² E-mail: waxman@wicc.weizmann.ac.il

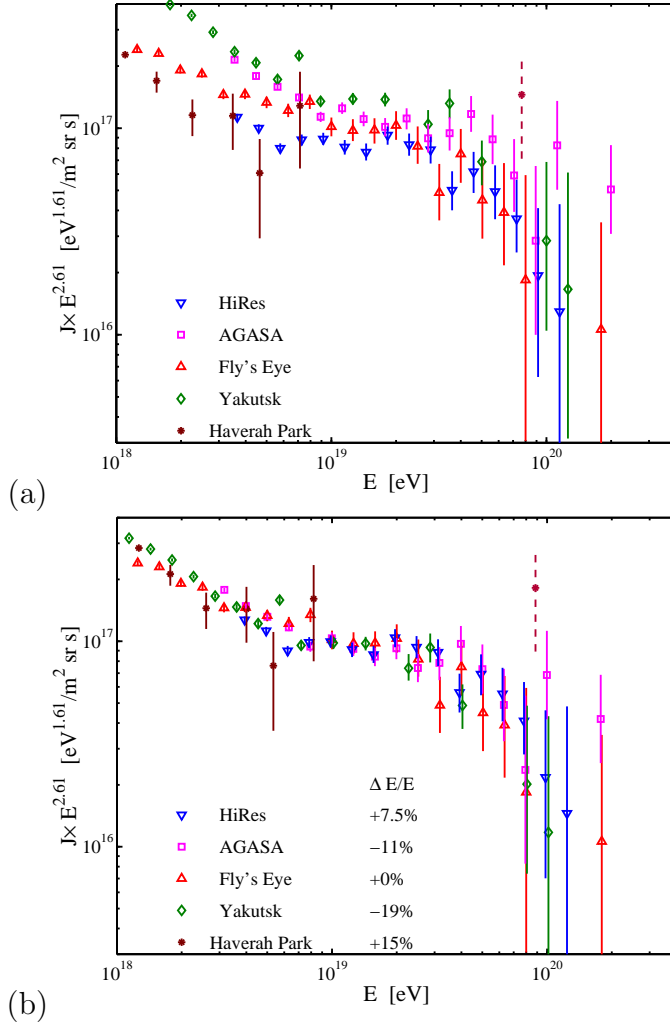


Fig. 1. Currently available data on the highest energy cosmic rays. The quantity J is the differential energy flux, $d\phi/dE$, per unit time per unit area per steradian. Panel (a) shows the data as published by the five experimental collaborations: AGASA [1], Fly’s Eye [2], Haverah Park [3], HiRes [4], and Yakutsk [5]. Panel (b) shows the data after adjusting the absolute energy calibrations of the various experiments so as to bring the results from the different experiments into agreement at 10^{19} eV. For specificity, the Fly’s Eye absolute energy scale was adopted as the standard. The fractional shifts in absolute energy scale, $\Delta E/E$, shown in the figure, are all well within the published systematic errors in the energy scale.

are consistent with a GZK suppression implies that the observed spectrum is consistent with model predictions for a plausible intrinsic energy spectrum. In particular, we show that the observed spectrum is consistent with that expected for a GZK suppression of the flux produced by a simple cosmological distribution of sources, each source producing high energy protons with a spectrum $dN/dE_p \propto E_p^{-2}$ characteristic for collisionless shock acceleration.

Before entering into any details, we will summarize and compare in this introduction the data that are available from different collaborations that measure

the spectrum of ultra high energy cosmic rays.

1.1 Summary of available data

Figure 1 is a "Before-After" figure of the currently available data on the highest energy cosmic rays (energies $> 10^{18}$ eV). In Figure 1a (the "Before" version of the figure), the data are plotted, together with their flux error bars, as they have been published by the five experimental collaborations: AGASA [1], Fly's Eye [2], Haverah Park [3], HiRes [4], and Yakutsk [5]. The Haverah Park data have recently been re-analyzed using modern numerical simulations of air-shower development [3]. The reanalysis resulted in significant changes of inferred cosmic-ray energies compared to previously published results ([6] and references quoted therein). The data points for the Haverah Park measurements that are shown in Fig. 1 are based on this improved analysis, which is available only at energies $< 10^{19}$ eV³.

The most striking feature of Figure 1a is that the experimental results differ greatly among themselves (by factors ~ 2) even in the region 10^{18} eV $< E < 2 \times 10^{19}$ eV, where the quoted error bars from each experiment are very small. In addition, the higher AGASA flux reported above 2×10^{20} eV stands out above the scatter in the different experimental measurements.

Figure 1b (the "After" version of our "Before-After" figure) shows a dramatically different representation of the available data. With small adjustments in the absolute energy scales, all of the measured fluxes are seen to be in agreement at energies below 10^{20} eV. In constructing Figure 1b, we have adjusted the absolute energy calibrations within the error bars published by the experimental collaborations. We chose the shifts so as to bring the different measured fluxes into agreement at 10^{19} eV. The energy shifts can be accomplished in five equivalent ways, depending upon which one of the five energy scales is unaltered. For Figure 1b, the Fly's Eye energy scale was unaltered and we adjusted the AGASA energy scale by -11%, Haverah Park by +15%, HiRes by +7.5%, and Yakutsk by -19%. All shifts are well within the published systematic errors.

Figure 1 illustrates visually our two main points. First, all of the currently

³ A single flux point at $\sim 7 \times 10^{19}$ eV is shown in Figure 1a, but this point is based on a preliminary analysis of 4 events that are chosen by different cuts than those applied for the lower energy data. The energy uncertainty for the point at $\sim 7 \times 10^{19}$ eV is significantly larger than the estimated uncertainties for lower energy points [3]. Therefore, the point at $\sim 7 \times 10^{19}$ eV is shown in Figure 1a only for completeness; it is not used elsewhere in our analysis because the Haverah Park collaboration has described this point as preliminary.

available data on high energy cosmic rays are in agreement within their quoted errors for energies between 2×10^{18} eV and 10^{20} eV. Second, three of the four data sets available above 10^{19} eV, HiRes, Fly's Eye, and Yakutsk, all show evidence for a turnover of the energy spectrum for energies above 5×10^{19} eV. This turnover, we shall show later, is highly significant statistically and is consistent with what one would expect from a simple model that includes the GZK effect. Above 10^{20} eV, the reported AGASA fluxes are higher than the fluxes measured in other experiments. It is these high AGASA fluxes alone that have led to the widespread impression that measurements of ultra-high energy (UHE) cosmic rays (energies $> 10^{19}$ eV) do not show evidence for a GZK effect.

1.2 What does it all mean?

What can one make of the results shown in the Before-After Figure 1? There are two simple possibilities. First, the excellent agreement shown in Figure 1b among the different experiments could be accidental. According to this interpretation, the small adjustments made in the energy scales are not physically motivated and the real situation is somehow much more complicated. It is just a fluke that all of the adjusted energy spectra line up together so well below 10^{20} eV. This interpretation is certainly possible. In the present paper, however, we shall choose a different interpretation of Figure 1b. We shall suppose that the excellent agreement of the adjusted energy spectra reveals a good approximation to the true shape of the UHE cosmic ray energy spectra. We shall now explore the consequences of this assumption.

We stress that the distinction between the two possibilities for interpreting Figure 1b can only be settled by a new generation of precise and high statistics measurements of the UHE cosmic ray spectrum. Fortunately, the Auger experiment, currently under construction [7], is expected to provide the necessary precision and statistics. The Telescope Array experiment [8], currently under planning, may also provide similar precision and statistics.

We first describe in Section 2 the model we use and then in Section 3 we compare the model predictions with observations of the UHE cosmic ray energy spectrum. We summarize our main conclusions in Section 4.

2 A simple two-component model

We describe in this section a simple two-component model for the energy spectrum of the highest energy cosmic rays. The Galactic component is taken

from observations of the Fly’s Eye group. The two input parameters for the extra-galactic component (the rate of energy deposition in cosmic rays and the shape of the initial spectrum) were originally suggested by the idea [9–11] that gamma-ray bursts (GRBs) are the source of UHE cosmic rays. However, any postulated cosmologically distributed source of cosmic rays with a similar energy production rate and energy spectrum (Eq. 1 and 2 below) would yield agreement with the observations.

In order to avoid the risk of being misled by ”curve fitting”, we use the same theoretical model that was discussed in 1995 [12]. We assume that extra-galactic protons in the energy range of 10^{19} eV to 10^{21} eV are produced by cosmologically-distributed sources at a rate

$$\frac{d\varepsilon}{dt} \approx 3 \times 10^{44} \text{erg Mpc}^{-3} \text{ yr}^{-1}, \quad (1)$$

with a power law differential energy spectrum

$$\frac{dN}{dE_p} \propto E_p^{-n}, \quad n \approx 2. \quad (2)$$

We shall refer to this energy spectrum as “the extra-galactic component” in order to emphasize that the fit to the data is generic, independent of the type of source that generates the assumed energy and spectrum. An energy spectrum similar to the assumed energy spectrum, Eq. (2), has been observed for non-relativistic shocks [13] and for relativistic shocks [14] shocks. This power law is produced by Fermi acceleration in collisionless shocks [13], although a first principles understanding of the process is not yet available (see, e.g. Ref. [15] for a discussion of alternative shock acceleration processes).

We can use Eq. (1) and Eq. (2) to obtain a value for the cosmological rate, $E_p^2 d\dot{N}/dE_p$, at which energy in the form of high energy protons is being produced. Integrating $E_p d\dot{N}/dE_p$ between 10^{19} eV and 10^{21} eV and setting the result equal to the value given in Eq. (1), we find the proportionality constant in Eq. (2). Thus $E_p^2 d\dot{N}/dE_p \approx 0.7 \times 10^{44} \text{erg Mpc}^{-3} \text{ yr}^{-1}$.

Energy losses due to pion or pair production are included in the transport calculations in the usual continuous approximation. Energy loss due to the cosmological redshift is significant for energies $< 5 \times 10^{19}$ eV, and is also taken into account. The choice of cosmological model is unimportant for cosmic ray energies above 10^{19} eV, which is the region of interest. We assume, for definiteness, a flat universe with $\Omega_m = 0.3$ and $\Omega_\Lambda = 0.7$, and Hubble constant $H_0 = 65 \text{ km/s Mpc}$. For consistency with our earlier derivation of the upper bound on neutrino fluxes that follows from the observed cosmic ray spectrum [16], we assume that the source density evolves with redshift z

like the luminosity density evolution of QSOs [17], which may be described as $f(z) = (1+z)^\alpha$ with $\alpha \approx 3$ [18] at low redshift, $z < 1.9$, $f(z) = \text{Const.}$ for $1.9 < z < 2.7$, and an exponential decay at $z > 2.7$ [19]. This functional form of $f(z)$ is also similar [17] to that describing the evolution of star formation rate [20], and also believed to describe the redshift evolution of GRB rate (see, e.g. [21] for review). As mentioned above, the choice of redshift evolution does not affect the spectrum above 10^{19} eV.

The cosmic-ray spectrum flattens at $\sim 10^{19}$ eV [2,1]. There are indications that the spectral change is correlated with a change in composition, from heavy to light nuclei [2,22,23]. These characteristics, which are supported by analysis of Fly’s Eye, AGASA and HiRes-MIA data, and for which some evidence existed in previous experiments [6], suggest that the cosmic ray flux is dominated at energies $< 10^{19}$ eV by a Galactic component of heavy nuclei, and at UHE by an extra-Galactic source of protons. Also, both the AGASA and Fly’s Eye experiments report an enhancement of the cosmic-ray flux near the Galactic disk at energies $\leq 10^{18.5}$ eV, but not at higher energies [24].

We therefore add an observed Galactic component,

$$\frac{dN}{dE} \propto E^{-3.50}, \quad (3)$$

to the extra-galactic spectrum component given in Eq. (2). The shape of the energy spectrum of the Galactic component, Eq. (3), was derived by the Fly’s Eye collaboration [2].

The observed $E^{-2.6}$ spectrum between 1×10^{19} eV to 5×10^{19} eV is, in this model, the combination of two different source spectra. First, the cosmological distribution of sources generates an E^{-2} spectrum (see Eq. 2), which energy losses due to interactions with the CMB steepen to an observed spectrum that is a bit shallower than $E^{-2.6}$. Second, the Fly’s Eye fit to the Galactic heavy nuclei component makes a small contribution at energies $> 1 \times 10^{19}$ eV and is steeper than $E^{-2.6}$. We will now compare the model spectrum produced by these two sources with the cosmic ray observations.

3 Comparison of Model with Cosmic Ray data.

Figure 2 compares the model prediction with the data from the AGASA [1], Fly’s Eye [2], Hires [4], and Yakutsk [5] cosmic ray experiments. In order to demonstrate that our results are insensitive to the choice of absolute energy scale, we present results for three different choices of the absolute energy scale: adopting the Fly’s Eye, the AGASA or the Yakutsk energy calibration. The

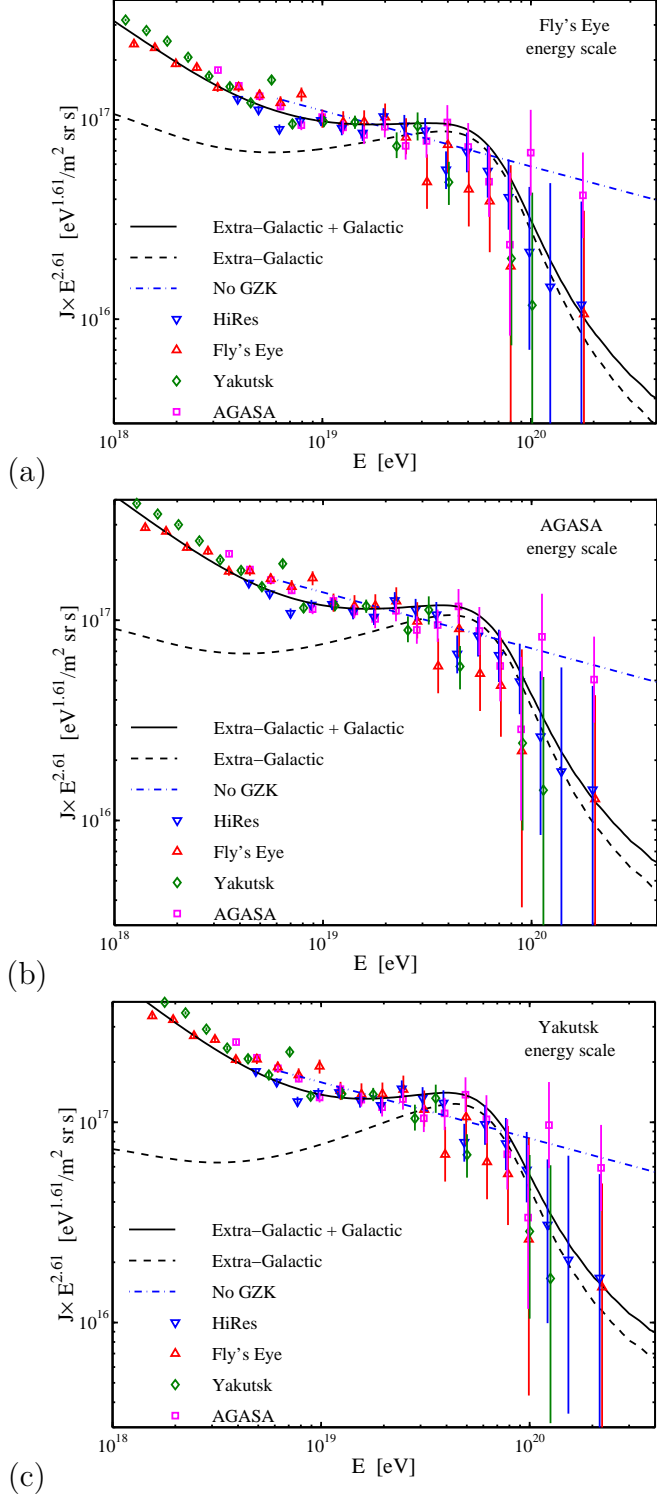


Fig. 2. Model versus data. The solid curve shows the energy spectrum derived from the two-component model discussed in Section 2. The dashed curve shows the extra-Galactic component contribution. The "No GZK" curve is an extrapolation of the $E^{-2.75}$ energy spectrum derived for the energy range of 6×10^{18} eV to 4×10^{19} eV ([25]; see text) . Three choices of the absolute energy scale are illustrated.

three best fit (solid) curves correspond to energy generation rates (see Eq. 1) of $d\varepsilon/dt = \{2.5, 3.0, 3.5\} \times 10^{44} \text{erg/Mpc}^3 \text{yr}$ and spectral indices, (see Eq. 2) of $n = \{-2.2, -2.1, -2.0\}$ for the {Fly’s Eye, AGASA, Yakutsk} energy scales, respectively.

3.1 Good agreement below 10^{20} eV

The model predictions are in good agreement with the data of all experiments in the energy range 10^{19} eV to 10^{20} eV, a region in which the extra-galactic component is predicted to be dominant. Since the Fly’s Eye representation of the Galactic component is intended to describe the lower energies, it is not surprising that the model results are also in good agreement with the observed spectrum for energies below 10^{19} eV.

A ” χ -by-eye” comparison of the model to the data shown in Figures 2 appears to indicate a quantitatively good fit, but we cannot simply compute a formal χ^2 fit due to the uncertainties in the absolute energy calibration. Instead, we compare the variance of model predictions from the combined AGASA, Fly’s Eye, HiRes and Yakutsk data sets (s_{Model}^2) with the variance of AGASA, Fly’s Eye, Haverah Park, and Yakutsk data sets from the HiRes data set (s_{HR}^2). Let $s_{\text{Model}}^2 \equiv N^{-1} \sum_{i,j} (n_{ij} - n_{ij,\text{Model}})^2 / n_{ij,\text{Model}}$ where $n_{ij,\text{Model}}$ is the predicted average number of events in the i -th energy bin of the j -th experiment and N is the number of bins. Also, let $s_{\text{HR}}^2 \equiv \tilde{N}^{-1} \sum_{i,j} (n_{ij} - n_{ij,\text{HR}})^2 / n_{ij,\text{HR}}$, where $n_{ij,\text{HR}}$ is the predicted average number of events (for AGASA, Fly’s Eye and Yakutsk) in a model where the HiRes value is the average number of events. We find $s_{\text{HR}}^2 = 1.06$ with $\tilde{N} = 26$ data points, and $s_{\text{Model}}^2 = 1.20$ with $N = 36$ data points for all three choices of the absolute energy scale (panels a, b or c). The different experiments are in agreement with each other and with the model in the energy range 10^{19} eV to 10^{20} eV.

3.2 What is happening above 10^{20} eV?

Above 10^{20} eV, Fig. 2 shows that the Fly’s Eye, HiRes and Yakutsk experiments are in agreement with each other and the model. However, the eight AGASA events with energies greater than 10^{20} eV disagree with the prediction of the cosmological model (defined by Eq. 1 and Eq. 2), including the GZK suppression. The Fly’s Eye, Yakutsk and HiRes experiments have a combined exposure three times that of the AGASA experiment. The exposures above 10^{20} eV are, in units of $10^3 \text{km}^2 - \text{yr} - \text{sr}$: AGASA (1.3), Fly’s Eye (0.9), Yakutsk (0.9), and HiRes (2.2). Together, Fly’s Eye, Yakutsk, and Hi-Res observe a total of 6 events above 10^{20} eV (4 events if the Fly’s Eye energy scale is chosen).

Table 1

Evidence for a GZK suppression. The table compares the number of events expected above 10^{20} eV assuming that there is no GZK suppression with the observed number of events for different choices of the absolute energy scale. The expected number of events is calculated assuming that the power law $J \propto E^{-2.75}$ that dominates between 6×10^{18} eV and 4×10^{19} eV [25] extends beyond 5×10^{19} eV. The numbers of events are given for the combined exposure of the Fly’s Eye, HiRes, and Yakutsk experiments.

Energy Scale	Expected	Observed
Fly’s Eye	34	4
AGASA	40	6
Yakutsk	46	6

Assuming no GZK suppression, Table 1 compares the expected number of events above 10^{20} eV with the number of events observed in the combined Fly’s Eye, HiRes, and Yakutsk exposure. The differential energy spectrum observed by the various experiments at the energy range of 4×10^{17} eV to 4×10^{19} eV can be fitted by a broken power-law, where the shallower component dominating above $\sim 6 \times 10^{18}$ eV satisfies $J \propto E^{-2.75 \pm 0.2}$ (see table V and Eq. 43 in [25]). The expected number of events in the absence of a GZK suppression was calculated by assuming that the cosmic ray spectrum follows the power law $J \propto E^{-2.75}$ also at energies $> 4 \times 10^{19}$ eV. Thus there is a $> 5\sigma$ deficit beyond 10^{20} eV relative to the extrapolated lower-energy spectral energy distribution. Adopting the steepest allowed slope, $J \propto E^{-2.95}$, the expected number of events is $\{21,25,30\}$, implying a $> 3.7\sigma$ deficit beyond 10^{20} eV .

4 Discussion.

Our most important conclusion is that exotic new physics is not required to account for the observed events with energies in excess of 10^{20} eV, except for the AGASA data. Table 1 shows that there is already a strong suggestion, $> 5\sigma$ ($> 3.7\sigma$, depending upon the extrapolated energy spectrum) in the Fly’s Eye, HiRes, and Yakutsk observations that the expected GZK suppression has been observed (see also Fig. 1 and Fig. 2).

Precision measurements from 10^{18} eV to 5×10^{19} eV are essential for testing models of UHE cosmic rays, although they are less dramatic than measurements above 10^{20} eV. At energies $> 10^{20}$ eV, the predicted number, N , of events in conventional models is uncertain due to the unknown clustering scale, r_0 , of the sources, $\sigma(N_{\text{predicted}})/N_{\text{predicted}} = 0.9(r_0/10 \text{ Mpc})^{0.9}$ [26]. Paradoxically, we may need to study carefully cosmic rays with energies below the

GZK suppression in order to understand better the origin of the cosmic rays beyond the suppression.

Acknowledgments

We are grateful to M. Teshima for valuable comments. JNB acknowledges NSF grant No. 0070928 and the WIS Einstein Center for hospitality. EW thanks the IAS for hospitality. EW is the incumbent of the Beracha foundation career development chair.

References

- [1] M. Takeda et al., Phys. Rev. Lett. 81 (1998) 1163; N. Hayashida et al., Astrophys. J. 522 (1999) 225 and astro-ph/0008102.
- [2] D.J. Bird et al., Phys. Rev. Lett. 71 (1993) 3401; D.J. Bird et al., Astrophys. J. 424 (1994) 491.
- [3] J. Hinton et al., Proc. Ultra High Energy Particles from Space, Aspen 2002 (<http://hep.uchicago.edu/~jah/aspden/aspden2.html>).
- [4] T. Abu-Zayyad et al., astro-ph/0208243.
- [5] N.N. Efimov et al., in the Proceedings of the International Symposium on Astrophysical Aspects of the Most Energetic Cosmic-Rays, edited by M. Nagano and F. Takahara (World Scientific, Singapore 1991), p. 20.
- [6] A.A. Watson, Nuc. Phys. B (Proc. Suppl.) 22 (1991) 116.
- [7] J.W. Cronin, Nucl. Phys. B (Proc. Suppl.) 28 (1992) 313.
- [8] M. Teshima et al., Nucl. Phys. B (Proc. Suppl.) 28 (1992) 169.
- [9] E. Waxman, Phys. Rev. Lett. 75 (1995) 386.
- [10] M. Vietri, Astrophys. J. 453 (1995) 883.
- [11] M. Milgrom and V. Usov, Astrophys. J. Lett. 449 (1995) L37.
- [12] E. Waxman, Astrophys. J. Lett. 452 (1995) L1.
- [13] R. Blandford, D., Eichler, Phys. Rep. 154 (1987) 1; J. Bednarz, M. Ostrowski, Phys. Rev. Lett. 80 (1998) 3911; A. Achterberg et al., MNRAS 328 (2001) 393.
- [14] E. Waxman, Astrophys. J. 485 (1997) L5.
- [15] J. Arons, M. Tavani, Astrophys. J. Supp. Series 90 (1994) 797.

- [16] J.N. Bahcall, E. Waxman, *Phys. Rev. D* 64 (2001) 023002.
- [17] B.J. Boyle, R.J. Terlevich, *MNRAS* 293 (1998) L49.
- [18] P.C. Hewett, C.B. Foltz, F. Chaffee, *Astrophys. J.* 406 (1993) 43.
- [19] M. Schmidt, D.P. Schneider, J.E. Gunn, *Astron. J.* 110 (1995) 68.
- [20] S.J. Lilly, O. Le Fevre, F. Hammer, D. Crampton, *Astrophys. J.* 460 (1996) L1; P. Madau, H.C. Ferguson, M.E. Dickinson, M. Giavalisco, C.C. Steidel, A. Fruchter, *MNRAS* 283 (1996) 1388.
- [21] P. Mészáros, *Science* 291 (2001) 79.
- [22] T.K. Gaisser et al., *Phys. Rev. D* 47 (1993) 1919; B.R. Dawson, R. Meyhandan, K.M. Simpson, *Astropart. Phys.* 9 (1998) 331.
- [23] T. Abu-Zayyad et al., *Astrophys. J.* 557 (2001) 686.
- [24] D.J. Bird et al., *Astrophys. J.* 511 (1998) 739; N. Hayashida et al., *Astropart. Phys.* 10 (1999) 303.
- [25] M. Nagano, A.A. Watson, *Rev. Mod. Phys.* 72 (2000) 689.
- [26] J.N. Bahcall, E. Waxman, *Astrophys. J.* 542 (2000) 542.